THE HIDDEN LATTICE GEOMETRY OF LLMS

Anonymous authors
Paper under double-blind review

ABSTRACT

We uncover the *hidden lattice geometry* of large language models (LLMs): a symbolic backbone that grounds conceptual hierarchies and logical operations in embedding space. Our framework unifies the *Linear Representation Hypothesis* with *Formal Concept Analysis (FCA)*, showing that linear attribute directions with separating thresholds induce a concept lattice via half-space intersections. This geometry enables symbolic reasoning through geometric meet (*intersection*) and join (*union*) operations, and admits a canonical form when attribute directions are linearly independent. Experiments on WordNet sub-hierarchies provide empirical evidence that LLM embeddings encode concept lattices and their logical structure, revealing a principled bridge between continuous geometry and symbolic abstraction.

1 INTRODUCTION

Large language models (LLMs) (Achiam et al., 2023; Grattafiori et al., 2024; Mesnard et al., 2024) are surprisingly effective in capturing conceptual knowledge (Petroni et al., 2019; Wu et al., 2023; Lin & Ng, 2022; Xiong & Staab, 2025) and performing logical reasoning, capabilities traditionally associated with symbolic AI. Yet, it remains fundamentally unclear how exactly such conceptual knowledge, including concepts, hierarchies, and their logical semantics, is encoded within the continuous geometry of LLM representation spaces. Unlocking this hidden geometry is crucial not only for interpreting how LLMS representing symbolic knowledge, but also for reliably controlling and steering their inference behavior (Han et al., 2024), a fundamental step for advancing AI safety.

To understand concept representations in LLMs, a promising direction is the *Linear Representation Hypothesis* (Mikolov et al., 2013b; Park et al., 2025; 2024a; Gurnee & Tegmark, 2024), which posits that semantic features and concepts are encoded as linear directions or subspaces in a model's embedding space. This idea, rooted in early work on word embeddings (Pennington et al., 2014a), has since been extended to modern LLMs, where such directions can be interpreted as embedding difference, logistic probing, or steering vectors in different contexts (Gurnee & Tegmark, 2024; Nanda et al., 2023; Zhao et al., 2025). Park et al. (Park et al., 2024a) unifies these them through *causal inner product* that respects the semantic structure of concepts in the sense that causally separable concepts are represented by orthogonal vectors. However, these works mainly focus on exploring the existence of the linearity of (binary) concepts, but offer limited insights for interpreting compositional or set-theoretic semantics such as concept inclusion, concept intersection, and union, which lies at the heart of symbolic abstraction.

Recently, Park et al. (Park et al., 2025) extended the Linear Representation Hypothesis to formalize *categorical concepts* as geometric regions like *polytopes* in the representation space, and show that semantic hierarchy corresponds to orthogonality. However, they model concepts purely in terms of their extensions, that is, as sets of tokens or objects that fall under the category, such as $Y(\texttt{animal}) = \{\texttt{predator}, \texttt{bird}, \texttt{dog}, \ldots\}$. While this extensional view is useful for evaluating membership, it overlooks their intensional nature, i.e., the attributes and relations that ground categories in logic and philosophy, making it difficult to interprete how concepts are related to each others through set-theoretic semantics like concept subsumption, intersection, or union.

We draw inspiration from Formal Concept Analysis (FCA) (Ganter et al., 2005), a principled and philosophy-inspired framework that defines concepts through both their instances and their attributes. In FCA, each concept is represented as a pair: an extent (the set of objects) and an intent (the set of shared attributes). For example, the concept bird may be defined by attributes such as can fly, has

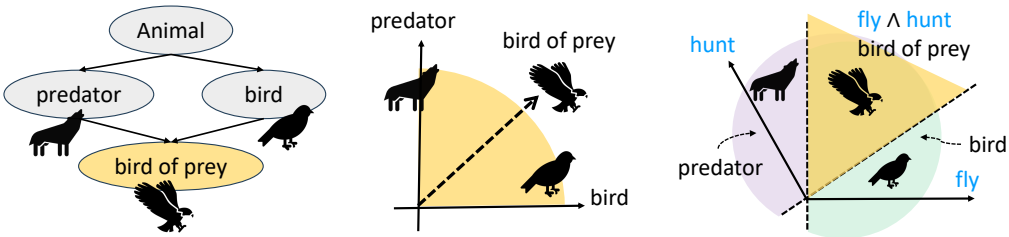

(a) Human view (b) Extensional view (c) Intensional view (ours)

Figure 1: **An illustration of how linear representation of LLMs induces conceptual structures.** (a) An example of concept hierarchy in human view; (b) Extensional view of the linear geometry inducing concept hierarchy, where hierarchy is captured by vector orthogonality; (c) The proposed intensional view of the linear geometry inducing concept hierarchy, where hierarchy is captured by region entailment and compositional semantics is captured by region intersection.

feathers, and lays eggs, while eagle (a bird of prey) refines this category by denoting a subset of birds with additional features such as can hunt. As Figure 1 shows, unlike extensional view defining concepts as instances, such dual intent-extent view defines concepts as convex regions bounded by their attributes defining them. For example, the concept *bird* may be defined by attributes like *can fly*, *has feathers*, and *lays eggs*, while *eagle* (a bird of prey) refines this category by denoting a subset of birds with additional features such as *can hunt*. This dual formulation naturally induces a concept lattice, because every pair of concepts can be ordered by inclusion of their extents (or, dually, their intents), and any two concepts have a well-defined intersection (their common subconcept) and union (their common superconcept), corresponding to the meet and join operations of the lattice.

In this work, we unify two perspectives on concept representation: the *Linear Representation Hypothesis*, which views semantics as directions in embedding geometry, and *Formal Concept Analysis*, which formalizes concepts through the incidence relation between objects and attributes. **Our key insight is that these views coincide, revealing a hidden lattice geometry in LLMs:** attribute directions correspond to FCA intents, object embeddings to extents, and symbolic abstractions such as subsumption, intersection, and union emerge naturally from the induced closure structure. Building on this connection, we formalize a half-space model of concepts and a projection-based notion of concept inclusion that together recover a lattice geometry from LLM representations. Our contributions are threefold: (i) a theoretical framework linking Linear Representation Hypothesis to FCA via half-space intersections, (ii) a soft inclusion measure and concept algebra (meet/join) defined directly on embeddings, and (iii) empirical evidence on WordNet sub-hierarchies showing that LLM embeddings encode concept lattices, enabling coherent generalization (join) and refinement (meet). These results demonstrate that LLMs implicitly organize conceptual knowledge into a lattice geometry, providing a symbolic backbone for interpretability and controllability.

2 Preliminaries

2.1 Linear Representation Hypothesis in LLMs

We consider the autoregressive family of LLMs that predict the next tokens given its context.

Definition 1 (Large Language Model)**.** *An LLM defines a probability distribution over the next token y given a context x via the softmax function $\Pr(y \mid x) \propto \exp\left(\lambda(x)^\top \gamma(y)\right)$, where $\lambda : \mathcal{X} \to \Lambda \simeq \mathbb{R}^d$ maps the input context x to a context embedding vector $\lambda(x)$, and $\gamma : \mathcal{V} \to \Gamma \simeq \mathbb{R}^d$ maps each vocabulary token y to its unembedding vector $\gamma(y)$.*

This definition involves a *context embedding space* Λ and a *token unembedding space* Γ, which together define the geometry of the softmax distribution. These two spaces can be unified via the *causal inner product* (Park et al., 2024a). Specifically, there exists an invertible matrix $A \in \mathbb{R}^{d\times d}$ and a constant vector $\bar{\gamma}_0 \in \mathbb{R}^d$ such that defining $g(y) := A\left(\gamma(y) - \bar{\gamma}_0\right)$ and $\ell(x) := A^{-\top}\lambda(x)$, reparameterizes token and context embeddings into a shared semantic space, where their interaction is captured by the Euclidean inner product $\ell(x)^\top g(y)$. This transformation preserves the model's output distribution, as the softmax $\Pr(y \mid x)$ remains invariant under any choice of A and $\bar{\gamma}_0$.

In this unified space, Linear Representation Hypothesis states that certain semantic attributes correspond to specific directions. There is an explicit definition for binary attributes.

Definition 2 (Linear representation of a binary attribute/concept (Park et al., 2024a))**.** *A vector $\bar{\ell}_m \in \mathbb{R}^d$ is said to linearly represent a binary attribute $m \in \{0, 1\}$ if, for all context embeddings $\ell \in \mathbb{R}^d$, all scalars $\alpha > 0$, and all attributes $z \neq m$ that are causally separable from m, the following conditions hold:*

- ***Attribute activation:*** $\Pr(m = 1 \mid \ell + \alpha\bar{\ell}_m) > \Pr(m = 1 \mid \ell)$*;*
- ***Causal selectivity:*** $\Pr(z \mid \ell + \alpha\bar{\ell}_m) = \Pr(z \mid \ell)$.

In other words, moving in the direction $\bar{\ell}_m$ increases the likelihood of the attribute m without affecting any causally unrelated attributes. The direction merely encodes the semantic direction of the attribute, not its strength, as any positive scalar multiple $\alpha\bar{\ell}_m$ has the same qualitative effect.

2.2 Formal Concept Analysis (FCA)

FCA (Ganter et al., 2003) is a mathematical framework for modeling concepts as structured relationships between objects and their attributes. Unlike extensional views that define concepts simply as sets of objects (as in (Cowsik et al., 2024)), FCA treats a concept as an intensional abstraction: a set of objects characterized by a common set of attributes. This duality between objects and attributes allows FCA to capture both the semantic content of a concept and its compositional structure. FCA begins with a binary relation between objects and attributes, formalized as a *formal context*:

Definition 3 (Formal context)**.** *A formal context is a triple (G, M, I), where G is a finite set of objects, M is a finite set of attributes, and $I \subseteq G \times M$ is a binary relation (called the* incidence relation*) such that $(g, m) \in I$ indicates that object $g \in G$ possesses attribute $m \in M$.*

From this, FCA defines concepts as maximal sets of objects and attributes that are mutually consistent:

Definition 4 (Formal concept)**.** *Given a formal context (G, M, I), define the Galois connections as $A' := \{m \in M \mid \forall g \in A,\ (g, m) \in I\}$, $B' := \{g \in G \mid \forall m \in B,\ (g, m) \in I\}$. The pair (A, B) is a* formal concept *if and only if $A' = B$ and $B' = A$, where A is called the* extent *and B the* intent*.*

The set of formal concepts is partially ordered by inclusion of extents (i.e., $A_1 \subseteq A_2$) or equivalently by reverse inclusion of intents (i.e., $B_2 \subseteq B_1$).

Definition 5 (Concept lattice)**.** *Let (A_1, B_1) and (A_2, B_2) be formal concepts. Then $(A_1, B_1) \leq_C (A_2, B_2)$ if and only if $A_1 \subseteq A_2$ (equivalently, $B_2 \subseteq B_1$), where $\leq_C$ denotes the partial order relationship. Under the partial order $\leq_C$, the set of all formal concepts forms a complete lattice: every subset concepts have a greatest lower bound (*meet*) and a least upper bound (*join*).*

3 The Lattice Geometry in LLMs

We now establish a connection between the Linear Representation Hypothesis and Formal Concept Analysis (FCA), showing that the linear geometry of LLM embeddings gives rise to a concept lattice. The key idea is that each binary attribute can be modeled as a direction in the unified space, with membership approximated by a thresholded inner product. This naturally induces a binary object–attribute relation, from which a formal context and concept lattice can be constructed. We refer to this construction as the *lattice geometry* of LLMs. Fig. 2 illustrates such correspondence.

3.1 From Linear to Lattice Geometry

Geometric interpretation of attribute membership. Under the Linear Representation Hypothesis, semantic attributes are encoded as directions while objects (tokens or contexts) are encoded as vectors. Let $\bar{\ell}_m \in \mathbb{R}^d$ denote the direction for attribute m, and $\mathbf{v}_g \in \mathbb{R}^d$ the embedding of object g. The extent to which g possesses m can be estimated by the projection $\mathbf{v}_g \cdot \bar{\ell}_m$. In the idealized case, there exists a threshold τ_m such that $m(g) = 1 \iff \mathbf{v}_g \cdot \bar{\ell}_m \geq \tau_m$. However, perfect separation rarely holds in practice, so we define a *soft incidence relation*:

$$P_\alpha(m(g) = 1) := \sigma\big(\alpha \cdot (\mathbf{v}_g \cdot \bar{\ell}_m - \tau_m)\big)\,, \tag{1}$$

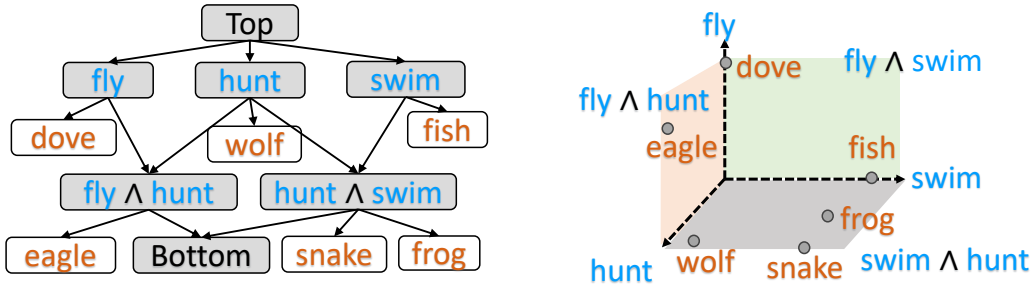

(a) Discreate Concept Lattice (b) Lattice geometry in LLMs

Figure 2: **An illustration of how LLMs encode concept lattice.** (a) Discrete concept lattice from the object-attribute incidence; (b) The lattice geometry induced from the linear attribute representations.

where $\alpha > 0$ controls sharpness. As $\alpha \to \infty$, this recovers the hard-thresholded case. This assigns each object–attribute pair a fuzzy degree of membership, enabling smoother definitions of concepts.

Theorem 1 (Existence of Lattice Geometry)**.** *Let G be a finite set of objects and M a finite set of attributes. Let $V = \{\mathbf{v}_g \in \mathbb{R}^d \mid g \in G\}$ be object embeddings and $\mathcal{D} = \{\bar{\ell}_m \in \mathbb{R}^d \mid m \in M\}$ attribute directions. Suppose for each $m \in M$ there exists a threshold $\tau_m \in \mathbb{R}$ such that membership is modeled by the soft incidence function above. For any confidence level $\delta \in (0, 1)$, define the binary incidence relation*

$$I_\delta := \{(\mathbf{v}_g, \bar{\ell}_m) \mid P_\alpha(m(g) = 1) \geq \delta\}.$$

Then the induced concept set

$$\mathcal{F}_\delta = \left\{ (X, Y) \,\middle|\, X = \{\mathbf{v} \in V \mid \forall \bar{\ell} \in Y, (\mathbf{v}, \bar{\ell}) \in I_\delta\},\ Y = \{\bar{\ell} \in \mathcal{D} \mid \forall \mathbf{v} \in X, (\mathbf{v}, \bar{\ell}) \in I_\delta\} \right\}$$

satisfies: (i) closure under the Galois connection, and (ii) forms a complete lattice under extent inclusion (equivalently, reverse intent inclusion). Proof is detailed in Appendix B.

Thus, when attributes are encoded as thresholded linear projections, a symbolic concept lattice can be recovered from embedding geometry, capturing semantic abstraction through graded boundaries.

Canonical representation under soft incidence. Theorem 1 allows arbitrary thresholds. We now show that under mild conditions, these thresholds can be absorbed into a global shift of embeddings, yielding a canonical origin-passing form:

Proposition 1 (Canonical representation)**.** *Let each attribute $m_i \in M$ be defined by direction $\mathbf{d}_i$ and threshold τ_i. Let $D \in \mathbb{R}^{k \times d}$ be the matrix with rows $\mathbf{d}_i^\top$, and $\boldsymbol{\tau} = (\tau_1, \ldots, \tau_k)$. If there exists $\mathbf{c} \in \mathbb{R}^d$ such that $D\mathbf{c} = \boldsymbol{\tau}$, then*

$$\sigma(\alpha(\mathbf{v}_g \cdot \mathbf{d}_i - \tau_i)) = \sigma(\alpha((\mathbf{v}_g - \mathbf{c}) \cdot \mathbf{d}_i)) \quad \forall g, i. \tag{2}$$

That is, the probabilities remain invariant under the transformation $\mathbf{v}_g \mapsto \mathbf{v}_g - \mathbf{c}$, reducing the model to a canonical half-space form while preserving the induced lattice. Proof is detailed in Appendix C.

3.2 Half-Space Model and Concept Algebra

Under the canonical representation, where all attribute thresholds have been absorbed via a global shift, each attribute defines an origin-passing half-space in the embedding space. A concept composed of multiple attributes can be interpreted geometrically as the intersection of those half-spaces, i.e., the region where all attribute constraints are simultaneously satisfied.

Definition 6 (Concept as half-space)**.** *Let M be a set of attributes, each represented by a direction $\mathbf{d}_m \in \mathbb{R}^d$. A concept defined by a subset $Y \subseteq M$ corresponds to the set of object embeddings that satisfy all associated directional constraints:*

$$\mathcal{R}(Y) := \left\{ \mathbf{v} \in \mathbb{R}^d \,\middle|\, \mathbf{v} \cdot \mathbf{d}_m \geq 0 \text{ for all } m \in Y \right\}. \tag{3}$$

Geometrically, $\mathcal{R}(Y)$ is a convex polyhedral cone defined by intersecting origin-passing half-spaces. However, this definition assumes perfect attribute separation, which may not hold in practice due to noise, uncertainty, and overlapping concept boundaries in LLM representations. To address this, we move from a hard region view to a *soft formulation*, where membership is modeled as graded alignment rather than binary inclusion.

Concept representation via normalized projection profiles. Given a concept C (e.g., a lexical term) and its associated context embeddings $\{\mathbf{v}_1, \ldots, \mathbf{v}_n\} \subset \mathbb{R}^d$, we define its semantic representation using the average projection profile over the attribute directions $\{\mathbf{d}_m\}_{m \in M}$. For each attribute $m \in M$, the projection value is

$$\pi_C(m) := \frac{1}{n} \sum_{i=1}^{n} \mathbf{v}_i \cdot \mathbf{d}_m. \tag{4}$$

The resulting projection vector $\boldsymbol{\pi}_C \in \mathbb{R}^{|M|}$ encodes a *soft attribute profile* of C, reflecting how strongly the concept aligns with each attribute. This can be seen as a continuous analogue of an FCA intent. To ensure comparability across concepts, all projection vectors are ℓ_2-normalized.

Concept inclusion as region containment. With projection profiles in place, we can now define a graded notion of subsumption between two concepts. Intuitively, a concept A is included in another concept B if the attributes emphasized by B are also strongly expressed in A. We capture this by a *soft inclusion score* that evaluates how well A's profile satisfies the attribute activations of B:

$$\text{Inclusion}(A \sqsubseteq B) = \frac{\sum_{m \in M} \phi(\pi_B(m)) \cdot \sigma(\pi_A(m))}{\sum_{m \in M} \phi(\pi_B(m))}, \quad \text{where} \quad \phi(x) = \log(1 + e^x). \tag{5}$$

Here, the sigmoid $\sigma(\cdot)$ maps A's projection value to a soft likelihood of satisfying attribute m, while the softplus $\phi(\cdot)$ weights attributes according to their salience in B. This formulation smoothly downweights weakly expressed or inactive attributes in B, while strongly positive ones dominate the inclusion score. Thus, concept inclusion is modeled not as a strict set-theoretic containment but as a continuous, geometry-driven compatibility measure between attribute profiles.

Concept Meet and Join. We operationalize concept algebra in the half-space model by defining meet and join directly on concept regions $\mathcal{R}(Y)$. Meet is the intersection of regions, while join is the least region subsuming both concepts, approximated by the conic hull of their defining directions.

Definition 7 (Concept algebra: meet and join)**.** *Let $\mathcal{R}(Y)$ denote the region associated with a concept defined by attribute set $Y \subseteq M$ (Definition 6).*

- ***Meet (intersection).*** *For two concepts $A = \mathcal{R}(Y_A)$ and $B = \mathcal{R}(Y_B)$, their meet is the region satisfying all attributes from both sets $A \wedge B := \mathcal{R}(Y_A \cup Y_B)$. Geometrically, this corresponds to intersecting the half-spaces that define A and B.*
- ***Join (union or generalization).*** *Their join is the least upper bound in the lattice, i.e., the most specific concept region that subsumes both A and B. In the half-space model, this corresponds to the minimal region that covers $\mathcal{R}(Y_A)$ and $\mathcal{R}(Y_B)$: $A \vee B := \mathcal{R}(Y_A) \cup \mathcal{R}(Y_B)$, which can be approximated by the conic hull spanned by the attribute directions of A and B.*

Soft measure of meet/join. While Definition 7 specifies meet and join geometrically, we also require a *graded* way to evaluate how well a concept C corresponds to these symbolic operations.

Soft meet/join profiles. Given two concepts A, B with projection profiles π_A, π_B, we define the projection profile of their meet and join using fuzzy t-norm/co-norm combinations:

$$\pi_{A \wedge B}(m) = \min\{\pi_A(m), \pi_B(m)\}, \qquad \pi_{A \vee B}(m) = \max\{\pi_A(m), \pi_B(m)\}. \tag{6}$$

Degrees of inclusion. The degree to which C is subsumed by the meet or join is

$$\deg(C \sqsubseteq A \wedge B) = \text{Inclusion}(C \sqsubseteq A \wedge B), \qquad \deg(C \sqsubseteq A \vee B) = \text{Inclusion}(C \sqsubseteq A \vee B), \tag{7}$$

where the inclusion function is as defined in Eq. (2).

Degrees of equality. Soft equality is defined by symmetrizing inclusion with the harmonic mean:

$$\deg(C = A \wedge B) = \frac{2\,\mathrm{Incl}(C \sqsubseteq A \wedge B) \cdot \mathrm{Incl}(A \wedge B \sqsubseteq C)}{\mathrm{Incl}(C \sqsubseteq A \wedge B) + \mathrm{Incl}(A \wedge B \sqsubseteq C)}, \tag{8}$$

$$\deg(C = A \vee B) = \frac{2\,\mathrm{Incl}(C \sqsubseteq A \vee B) \cdot \mathrm{Incl}(A \vee B \sqsubseteq C)}{\mathrm{Incl}(C \sqsubseteq A \vee B) + \mathrm{Incl}(A \vee B \sqsubseteq C)}. \tag{9}$$

4 Evaluation

In this section, we empirically evaluate the extent to which the linear structure of LLM embeddings induces a lattice geometry over concepts. We focus on testing the two core assumptions underlying our framework: 1) **Existence of half-space model:** How well do the linear representations of binary attributes recover the ground-truth formal context? 2) **Existence of lattice geometry in LLMs:** Does the approximated formal context recover a valid partial order set or concept lattice?

4.1 Dataset and Experiment Setup

Dataset construction. We construct three object–attribute datasets derived from the WordNet hierarchy: **WordNet-Animal**, **WordNet-Plant**, and **WordNet-Food** with each one corresponding to a distinct semantic domain. For each domain, we extract all concept terms that fall under the corresponding hierarchy using the WordNet `is_a` (hypernym) relation. We expand each concept by retrieving its synonyms and hyponyms to ensure lexical coverage and semantic granularity. Since WordNet does not provide explicit attribute annotations, we use a large language model (GPT-4o) to generate the attribute schema and populate the object–attribute matrix. Specifically, for each category, we first prompt the model to produce a concise set of salient binary attributes relevant to classification within the category (e.g., `can fly`, `has fur`, `lays eggs` for animals). We then use few-shot prompting to annotate each object with a binary attribute vector. This produces a complete binary incidence matrix, which we treat as the ground-truth *formal context* for evaluation. We use the WordNet `is_a` relation to define a symbolic subsumption hierarchy, and treat it as the target concept lattice structure. Using the annotated formal context and corresponding LLM embeddings for objects and attributes, we evaluate whether the geometry of the embedding space can reconstruct the symbolic structure implied by the context.

Object embedding. We represent each object g by averaging the embeddings of its synonymous lexical variants. Specifically, given a set of object names and their corresponding synonym sets, we compute the embedding for each synonym and define the object embedding as the mean over these representations $\mathbf{v}_g := \frac{1}{|\mathrm{Syn}(g)|} \sum_{s \in \mathrm{Syn}(g)} \mathrm{Emb}(s)$, where $\mathrm{Syn}(g)$ denotes the set of synonyms for object g, and $\mathrm{Emb}(s) \in \mathbb{R}^d$ is the vector embedding of synonym s. This procedure ensures more robust and semantically smoothed object representations by aggregating across synonymous variants.

Attribute embedding. To estimate the semantic direction associated with each attribute, we apply a linear discriminative analysis approach using object embeddings labeled as positive or negative with respect to that attribute. Given a set of positive and negative object embeddings for attribute m, we first compute the class means $\boldsymbol{\mu}_+$ and $\boldsymbol{\mu}_-$, and the class covariance matrices Σ_+ and Σ_-, estimated using Ledoit-Wolf shrinkage to improve robustness in high-dimensional settings. We then define the attribute direction $\bar{\ell}_m$ as the solution to a regularized Fisher separation criterion:

$$\bar{\ell}_m := (\Sigma_+ + \Sigma_- + \lambda I)^{-1} (\boldsymbol{\mu}_+ - \boldsymbol{\mu}_-), \tag{10}$$

where $\lambda > 0$ is a small regularization constant to ensure numerical stability. This procedure yields a direction vector that best separates the positive and negative object clusters in embedding space under a linear discriminant model. The resulting vector $\bar{\ell}_m$ is used as the attribute direction in all downstream projections and geometric reasoning.

Threshold estimation. Given an attribute direction $\bar{\ell}_m$, we determine a threshold $\tau_m \in \mathbb{R}$ to separate positive and negative objects along this direction. For each object embedding $\mathbf{v}_g$, we compute its projection onto the normalized direction, and then calculate the threshold as the average of the mean projections of positive and negative object sets:

$$\tau_m := \frac{1}{2} \left(\mathbb{E}_{g \in G_+} [\mathrm{Proj}_m(\mathbf{v}_g)] + \mathbb{E}_{g \in G_-} [\mathrm{Proj}_m(\mathbf{v}_g)] \right), \tag{11}$$

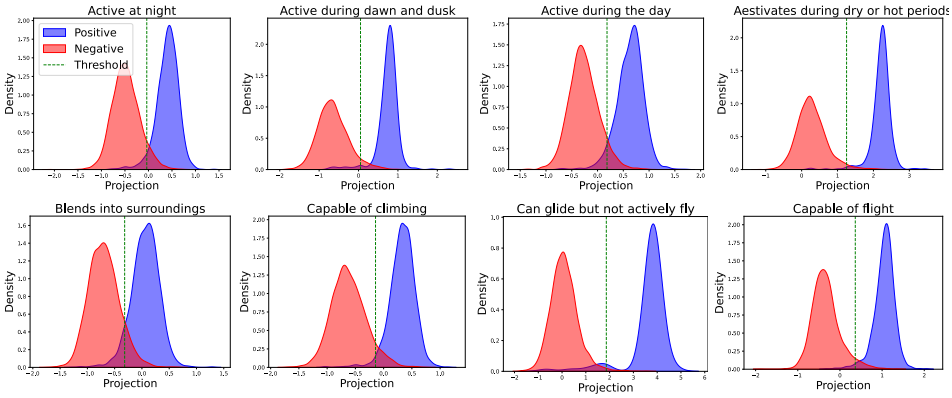

Figure 3: Distribution of projection lengths for positive and negative objects onto the directions of the first eight attributes (sorted alphabetically) in the WordNet-Animal dataset.

Table 1: Evaluation of linear representations for recovering concept–attribute relations (or formal context) across three WordNet domains. **Bold** values indicate the best performance across all models for a domain, while shading denotes the best method within each model. Metrics are reported as percentages for precision, recall, and F1 score.

Model		WN-Animal			WN-Plant			WN-Food		
		Pre.	Rec.	F1 S	Pre.	Rec.	F1	Pre.	Rec.	F1
Llama-3.1-8B	Random	49.7	49.6	45.3	501.	50.1	47.3	50.0	50.0	46.4
	Mean	63.7	69.3	63.7	63.7	67.2	63.3	67.2	71.4	68.1
	Linear	81.4	84.0	82.5	81.6	82.4	82.4	**79.7**	80.6	**80.1**
Gemma-7B	Random	49.8	49.7	45.3	50.1	50.1	47.3	50.1	50.1	46.3
	Mean	53.5	55.2	50.1	53.5	54.4	51.3	53.7	55.1	51.2
	Linear	**82.0**	**84.8**	**83.2**	**82.3**	**84.3**	**83.2**	79.2	**80.9**	80.0
Mistral-7B	Random	49.4	49.2	45.0	50.3	50.4	47.5	49.5	49.5	45.5
	Mean	62.2	67.1	62.0	61.9	64.9	61.4	62.4	66.6	62.1
	Linear	80.6	83.4	81.8	80.8	82.8	81.7	77.6	78.9	78.2

where G_+ and G_- denote the sets of positive and negative objects for attribute m, respectively. This threshold minimizes symmetric classification error under the assumption of linear separability and equal cost, and is used as the decision boundary in both hard and soft incidence models.

4.2 Existence of Half-Space Model

We first evaluate whether semantic attributes in LLM embedding space adhere to the half-space model—i.e., whether a single linear direction and threshold can reliably separate objects that possess a given attribute from those that do not. For each attribute m, we estimate a direction $\mathbf{d}_m$ and threshold τ_m using the training set (Section 4.1). Given an object embedding $\mathbf{v}_g$, we predict whether the object possesses the attribute using a hard decision rule $\hat{m}(g) = \mathbb{I}\left[\mathbf{v}_g \cdot \mathbf{d}_m \geq \tau_m\right]$, where $\mathbb{I}[\cdot]$ is the indicator function. We compare this prediction to the ground-truth incidence $m(g) \in \{0, 1\}$ from the annotated formal context. For each attribute, we compute precision, recall, and F1 score, and report averages over all attributes within each dataset.

Results. Table 1 reports the performance of different methods for recovering the formal context from LLM linear representations across three WordNet domains. The *Linear* method, which uses LDA to estimate attribute directions, consistently achieves the best F1 scores across all models and datasets—often exceeding 80% and peaking at 83.2% on both Animal and Plant domains for Gemma-7B. This confirms that attribute-level linear separation aligns strongly with ground-truth concept structure. The *Mean* baseline, which estimates directions by the difference between class centroids, performs moderately well with F1 scores around 62–68%. This indicates that class-level geometric trends are partially captured, but lack the discriminative power of supervised separation. In

Table 2: Evaluation of partial order inference from projection-based concept representations. **Bold** values indicate the best performance across all models for a domain, while shading denotes the best method within each model. Metrics are reported as percentages for precision, recall, and F1 score.

Model		WN-Animal			WN-Plant			WN-Food		
		Prec.	Rec.	F1	Prec.	Rec.	F1	Prec.	Rec.	F1
LLaMA-3.1-8B	Random	52.3	43.2	47.3	51.1	49.5	47.6	25.0	50.0	33.3
	Mean	68.4	65.0	66.7	64.2	63.3	63.8	61.5	58.5	55.7
	Linear	**75.9**	**78.3**	**77.1**	71.2	70.0	70.4	**78.1**	**75.9**	75.4
Gemma-7B	Random	54.0	51.2	50.6	52.7	50.3	49.5	53.4	50.8	39.1
	Mean	66.2	61.0	63.4	62.4	59.8	60.9	50.7	50.7	50.6
	Linear	74.4	76.0	75.1	72.9	**70.1**	**71.4**	76.3	75.8	**75.6**
Mistral-7B	Random	53.3	45.9	49.3	50.0	51.1	48.2	25.0	50.0	33.3
	Mean	66.8	63.4	64.9	61.2	60.0	60.5	56.0	55.6	54.8
	Linear	71.7	72.6	72.1	65.7	60.6	57.1	68.8	64.3	62.0

Table 3: Top-10 terms related to the join and meet of selected WordNet concept pairs.

A	**B**	**A** $\vee$ **B**	**A** $\wedge$ **B**
dog	wolf	predator, animal, canine, meat-eater, hunter, wild, mammal, quadruped, pet	dog, hound, puppy, terrier, mutt, beagle, retriever, spaniel, shepherd, pooch
cat	lion	predator, feline, animal, meat-eater, beast, carnivore, hunter, whiskers, mammal, wild	cat, kitten, tiger, panther, leopard, tomcat, feline, cheetah, tabby, lynx
sparrow	robin	avian, songbird, fowl, feathered, finch, beak, chirp, nest, perching, small	sparrow, robin, songbird, warbler, finch, canary, thrush, chickadee, pipit, titmouse
horse	zebra	equid, hoofed, animal, ungulate, mammal, quadruped, stallion, beast, herbivore	horse, pony, stallion, mare, foal, filly, mustang, gelding, thoroughbred, colt
carrot	parsnip	root, edible, produce, food, green, vegetable, crunchy, fresh, garden, plant	carrot, parsnip, radish, beet, turnip, tuber, rootcrop, veg, sprout, crop
eagle	falcon	animal, raptor, bird, predator, creature, wingspan, talon, flyer, sky, sharp-eyed	eagle, falcon, hawk, osprey, kestrel, buzzard, kite, harrier, condor, bird of prey

contrast, the *Random* baseline produces F1 scores near 45–47%, validating that attribute detection is not a trivial task and requires principled geometric alignment. Among models, Gemma-7B achieves the highest F1 on two of three domains, suggesting particularly strong encoding of symbolic concept structure. LLaMA-3.1-8B and Mistral-7B also show consistent performance, with LDA-based linear projections reliably reconstructing the formal context. Overall, the results provide strong empirical evidence that the linear structure of LLM embeddings supports the half-space model of concepts introduced in Section 3.2. We visualize the projection length distributions of positive and negative object embeddings for the first 8 attributes (sorted alphabetically) from WordNet-Animal. These density plots in Figure 3 show that a clear margin emerges around the estimated threshold, reinforcing the claim that LLM representations admit a thresholding scheme over directional projections.

4.3 Existence of lattice geometry

To test the *existence of lattice geometry*, we use the concept inclusion score defined in Section 3.2, where projection profiles over attribute directions are compared via the soft inclusion formula. This allows us to infer subsumptions directly from embedding geometry without access to ground-truth hierarchies. As Table 2 shows, the LINEAR method consistently outperforms centroid-based (MEAN) and random baselines across all domains, achieving F1 scores up to 77.1 (LLaMA, WN-Animal) and 75.6 (Gemma, WN-Food). These gains demonstrate that discriminatively estimated attribute directions capture intensional information sufficient to recover hierarchical relations: concepts with stronger projection activation on the attributes of another concept are reliably inferred as subconcepts. The empirical alignment between projection-based subsumption and WordNet ground-truth provides strong evidence that LLM embeddings indeed admit a partial order structure, supporting our hypothesis that lattice geometry is embedded within their representation space.

Qualitative Evaluation of Concept Algebra To qualitatively evaluate the concept algebra introduced in Section 3.2, we apply the soft measure of meet and join defined above to pairs of concepts and inspect the top-ranked terms associated with the resulting profiles.

Table 4.3 illustrates how these operations in embedding space yield semantically meaningful generalizations and refinements. The *join* operation ($A \vee B$) consistently surfaces higher-level abstractions that subsume both input concepts, e.g., *predator* for *dog* and *wolf*, or *avian* for *sparrow* and *robin*. These outputs align with WordNet hypernyms, confirming that the lattice geometry induces natural generalization. Conversely, the *meet* operation ($A \wedge B$) sharpens category boundaries by retrieving specific shared instantiations, such as *pony*, *stallion*, and *foal* for *horse* and *zebra*, or *hawk* and *osprey* for *eagle* and *falcon*. These intersective refinements capture fine-grained commonality, reflecting how logical conjunction is realized geometrically as half-space intersection. Together, these results provide qualitative evidence that concept joins and meets in LLM embeddings not only operate coherently but also mirror symbolic set-theoretic semantics. This supports our hypothesis that LLMs embed a latent lattice structure that can be harnessed for compositional reasoning.

5 Related Work and Discussion

Conceptual Knowledge in Language Models. Pretrained language models (LMs) have demonstrated remarkable capabilities in capturing conceptual knowledge (Wu et al., 2023; Lin & Ng, 2022). A variety of methods have been developed to probe such knowledge, most commonly binary probing classifiers (Aspillaga et al., 2021; Michael et al., 2020) and hierarchical clustering (Sajjad et al., 2022; Hawasly et al., 2024), with validation against human-defined ontologies such as WordNet (Miller, 1995). These approaches primarily provide empirical insights into what LMs capture, but they leave open the question of how LMs learn such conceptual structures. Moreover, it has been argued that LMs can develop novel concepts not strictly aligned with existing ontologies (Dalvi et al., 2022), suggesting that ontology-based evaluations may underestimate their conceptual capacity. Xiong & Staab (2025) first show the connection of FCA to language models by define concepts in the context of FCA, but their study is limited to masked language models.

Linear Representation Geometry of Concepts. A line of research focuses on the geometric nature of concept representations. Several studies suggest that concepts in LMs correspond to distinct directions in activation space (Elhage et al., 2022a; Park et al., 2024a). This linear hypothesis builds on earlier work in distributional semantics and embeddings (Mikolov et al., 2013a; Pennington et al., 2014b; Arora et al., 2016), and has since been connected to multiple notions of linearity, including embedding offsets, probing classifiers, and steering vectors (Park et al., 2024b). Empirical studies have also shown the emergence of polytopes in toy models (Elhage et al., 2022b), pointing to a more structured geometry beyond individual directions. Other theoretical work further explores why linear representations arise, linking them to properties of word embedding models (Arora et al., 2016; 2018) and the implicit bias of gradient descent in LLM training (Jiang et al., 2024).

6 Conclusion

We presented a new perspective on the geometry of large language models by linking the linear representation of attributes to Formal Concept Analysis (FCA). Our main contribution is the notion of *lattice geometry*, which shows that when attribute directions are treated as separating half-spaces, the resulting object–attribute relation induces a concept lattice. This framework unifies continuous embedding geometry with symbolic abstraction, and provides formal conditions under which logical structure can be recovered from LLM representations. Empirically, we demonstrated on WordNet sub-hierarchies that (i) many attributes are linearly separable, (ii) subsumption can be predicted directly from projection profiles, and (iii) meet and join operations yield meaningful refinements and generalizations. Together, these findings indicate that LLMs encode not only rich conceptual knowledge but also the algebraic backbone of concept lattices. Our results suggest that symbolic abstraction is not an incidental byproduct but a structured geometric property of LLMs. This opens up new directions for neuro-symbolic AI: aligning geometric and symbolic reasoning, enhancing interpretability, and enabling controllable manipulation of concepts in embedding space.

Ethics Statement

This work does not involve human subjects or sensitive personal data. Our experiments are conducted on publicly available lexical resources (WordNet) and pretrained LLM embeddings. We follow the ICLR Code of Ethics[1].

Reproducibility Statement

We have made efforts to ensure the reproducibility of our results. The formal definitions, theorems, and proofs are fully detailed in the main text and appendix. Experimental settings, dataset construction (WordNet sub-hierarchies and attribute annotation), attribute direction estimation, and evaluation metrics are described in Section 4. Detailed proofs are provided in the Appendix. Code for reproducing the experiments, including dataset processing and evaluation, are uploaded and will be made available in the supplementary materials.

References

Josh Achiam, Steven Adler, Sandhini Agarwal, Lama Ahmad, Ilge Akkaya, Florencia Leoni Aleman, Diogo Almeida, Janko Altenschmidt, Sam Altman, Shyamal Anadkat, et al. Gpt-4 technical report. *arXiv preprint arXiv:2303.08774*, 2023.

Sanjeev Arora, Yuanzhi Li, Yingyu Liang, Tengyu Ma, and Andrej Risteski. A latent variable model approach to pmi-based word embeddings. *Transactions of the Association for Computational Linguistics*, 4:385–399, 2016.

Sanjeev Arora, Yuanzhi Li, Yingyu Liang, Tengyu Ma, and Andrej Risteski. Linear algebraic structure of word senses, with applications to polysemy. *Transactions of the Association for Computational Linguistics*, 6:483–495, 2018.

Carlos Aspillaga, Marcelo Mendoza, and Alvaro Soto. Inspecting the concept knowledge graph encoded by modern language models. In *ACL/IJCNLP (Findings)*, volume ACL/IJCNLP 2021 of *Findings of ACL*, pp. 2984–3000. Association for Computational Linguistics, 2021.

Aditya Cowsik, Kfir Dolev, and Alex Infanger. The persian rug: solving toy models of superposition using large-scale symmetries. *CoRR*, abs/2410.12101, 2024.

Fahim Dalvi, Abdul Rafae Khan, Firoj Alam, Nadir Durrani, Jia Xu, and Hassan Sajjad. Discovering latent concepts learned in BERT. In *ICLR*. OpenReview.net, 2022.

Nelson Elhage, Tristan Hume, Catherine Olsson, Nicholas Schiefer, Tom Henighan, Shauna Kravec, Zac Hatfield-Dodds, Robert Lasenby, Dawn Drain, Carol Chen, Roger Grosse, Sam McCandlish, Jared Kaplan, Dario Amodei, Martin Wattenberg, and Christopher Olah. Toy models of superposition. *CoRR*, abs/2209.10652, 2022a.

Nelson Elhage, Tristan Hume, Catherine Olsson, Nicholas Schiefer, Tom Henighan, Shauna Kravec, Zac Hatfield-Dodds, Robert Lasenby, Dawn Drain, Carol Chen, et al. Toy models of superposition. *arXiv preprint arXiv:2209.10652*, 2022b.

Bernhard Ganter, Gerd Stumme, and R Wille. Formal concept analysis: Methods, and applications in computer science. *TU: Dresden, Germany*, 2003.

Bernhard Ganter, Gerd Stumme, and Rudolf Wille. *Formal concept analysis: foundations and applications*, volume 3626. springer, 2005.

Aaron Grattafiori, Abhimanyu Dubey, Abhinav Jauhri, Abhinav Pandey, Abhishek Kadian, Ahmad Al-Dahle, Aiesha Letman, Akhil Mathur, Alan Schelten, Alex Vaughan, et al. The llama 3 herd of models. *arXiv preprint arXiv:2407.21783*, 2024.

Wes Gurnee and Max Tegmark. Language models represent space and time. In *ICLR*. OpenReview.net, 2024.

[1] https://iclr.cc/public/CodeOfEthics

Chi Han, Jialiang Xu, Manling Li, Yi Fung, Chenkai Sun, Nan Jiang, Tarek F. Abdelzaher, and Heng Ji. Word embeddings are steers for language models. In *ACL (1)*, pp. 16410–16430. Association for Computational Linguistics, 2024.

Majd Hawasly, Fahim Dalvi, and Nadir Durrani. Scaling up discovery of latent concepts in deep NLP models. In *EACL (1)*, pp. 793–806. Association for Computational Linguistics, 2024.

Yibo Jiang, Goutham Rajendran, Pradeep Ravikumar, Bryon Aragam, and Victor Veitch. On the origins of linear representations in large language models. In *Proceedings of the 41st International Conference on Machine Learning (ICML)*, 2024.

Ruixi Lin and Hwee Tou Ng. Does BERT know that the IS-A relation is transitive? In *ACL (2)*, pp. 94–99. Association for Computational Linguistics, 2022.

Thomas Mesnard, Cassidy Hardin, Robert Dadashi, Surya Bhupatiraju, Shreya Pathak, Laurent Sifre, Morgane Rivière, Mihir Sanjay Kale, Juliette Love, et al. Gemma: Open models based on gemini research and technology. *arXiv preprint arXiv:2403.08295*, 2024.

Julian Michael, Jan A. Botha, and Ian Tenney. Asking without telling: Exploring latent ontologies in contextual representations. In *EMNLP (1)*, pp. 6792–6812. Association for Computational Linguistics, 2020.

Tomáš Mikolov, Wen tau Yih, and Geoffrey Zweig. Linguistic regularities in continuous space word representations. In *Proceedings of NAACL-HLT*, pp. 746–751, 2013a.

Tomás Mikolov, Wen-tau Yih, and Geoffrey Zweig. Linguistic regularities in continuous space word representations. In *HLT-NAACL*, pp. 746–751. The Association for Computational Linguistics, 2013b.

George A. Miller. Wordnet: A lexical database for english. *Commun. ACM*, 38(11):39–41, 1995.

Neel Nanda, Andrew Lee, and Martin Wattenberg. Emergent linear representations in world models of self-supervised sequence models. In *BlackboxNLP@EMNLP*, pp. 16–30. Association for Computational Linguistics, 2023.

Kiho Park, Yo Joong Choe, and Victor Veitch. The linear representation hypothesis and the geometry of large language models. *ICML*, 2024a.

Kiho Park, Yo Joong Choe, and Victor Veitch. The linear representation hypothesis and the geometry of large language models. In *Proceedings of the 41st International Conference on Machine Learning (ICML)*, 2024b.

Kiho Park, Yo Joong Choe, Yibo Jiang, and Victor Veitch. The geometry of categorical and hierarchical concepts in large language models. *ICLR*, 2025.

Jeffrey Pennington, Richard Socher, and Christopher D. Manning. Glove: Global vectors for word representation. In *EMNLP*, pp. 1532–1543. ACL, 2014a.

Jeffrey Pennington, Richard Socher, and Christopher D. Manning. Glove: Global vectors for word representation. In *Proceedings of the 2014 Conference on Empirical Methods in Natural Language Processing (EMNLP)*, pp. 1532–1543, 2014b.

Fabio Petroni, Tim Rocktäschel, Sebastian Riedel, Patrick S. H. Lewis, Anton Bakhtin, Yuxiang Wu, and Alexander H. Miller. Language models as knowledge bases? In *EMNLP/IJCNLP (1)*, pp. 2463–2473. Association for Computational Linguistics, 2019.

Hassan Sajjad, Nadir Durrani, Fahim Dalvi, Firoj Alam, Abdul Rafae Khan, and Jia Xu. Analyzing encoded concepts in transformer language models. In *NAACL-HLT*, pp. 3082–3101. Association for Computational Linguistics, 2022.

Weiqi Wu, Chengyue Jiang, Yong Jiang, Pengjun Xie, and Kewei Tu. Do plms know and understand ontological knowledge? In *ACL (1)*, pp. 3080–3101. Association for Computational Linguistics, 2023.

Bo Xiong and Steffen Staab. From tokens to lattices: Emergent lattice structures in language models. In *The Thirteenth International Conference on Learning Representations*, 2025.

Haiyan Zhao, Heng Zhao, Bo Shen, Ali Payani, Fan Yang, and Mengnan Du. Beyond single concept vector: Modeling concept subspace in llms with gaussian distribution. In *The Thirteenth International Conference on Learning Representations*, 2025.

A USE OF LARGE LANGUAGE MODELS (LLMS)

Large language models (LLMs) were only used as a writing assistant to polish sentences and improve clarity of exposition. No parts of the research ideation, theoretical development, experimental design, or analysis relied on LLMs. All technical contributions, proofs, and empirical results are the work of the authors.

B APPENDIX: PROOF OF THEOREM 1

We restate the theorem for convenience.

Theorem 2 (Existence of Lattice Geometry)**.** *Let G be a finite set of objects and M a finite set of attributes. Let $V = \{\mathbf{v}_g \in \mathbb{R}^d \mid g \in G\}$ be the set of object embeddings and $\mathcal{D} = \{\bar{\ell}_m \in \mathbb{R}^d \mid m \in M\}$ the set of attribute directions. Fix $\alpha > 0$. For each $m \in M$, let $\tau_m \in \mathbb{R}$ and define the soft incidence probability*

$$P_\alpha(m(g) = 1) := \sigma\big(\alpha(\mathbf{v}_g \cdot \bar{\ell}_m - \tau_m)\big).$$

For any confidence level $\delta \in (0, 1)$, define the (crisp) incidence relation

$$I_\delta := \{(g, m) \in G \times M : P_\alpha(m(g) = 1) \geq \delta\}.$$

Let $\mathcal{F}_\delta$ be the set of pairs (X, Y) with $X \subseteq G$ and $Y \subseteq M$ such that

$$X = Y' := \{g \in G : \forall m \in Y,\ (g, m) \in I_\delta\} \quad \text{and} \quad Y = X' := \{m \in M : \forall g \in X,\ (g, m) \in I_\delta\}.$$

Then (i) $\mathcal{F}_\delta$ is closed under the Galois connection, and (ii) $\mathcal{F}_\delta$, ordered by extent inclusion (equivalently, reverse intent inclusion), forms a complete lattice.

Plan of the proof. The probabilistic scoring is only used to induce the crisp relation I_δ. Once I_δ is fixed, the statement becomes a standard FCA result. For completeness, we give a self-contained proof.

B.1 GALOIS CONNECTION INDUCED BY I_δ

Lemma 1 (Antitone Galois connection)**.** *Define maps $(\cdot)' : 2^G \to 2^M$ and $(\cdot)' : 2^M \to 2^G$ by*

$$A' := \{m \in M : \forall g \in A,\ (g, m) \in I_\delta\}, \qquad B' := \{g \in G : \forall m \in B,\ (g, m) \in I_\delta\}.$$

Then for all $A \subseteq G$ and $B \subseteq M$, we have

$$A \subseteq B' \iff B \subseteq A'.$$

Consequently, both primes are antitone: if $A_1 \subseteq A_2$ then $A_2' \subseteq A_1'$, and if $B_1 \subseteq B_2$ then $B_2' \subseteq B_1'$.

Proof. ($\Rightarrow$) If $A \subseteq B'$, then for any $m \in B$ and any $g \in A$ we have $(g, m) \in I_\delta$, hence $m \in A'$ and thus $B \subseteq A'$. ($\Leftarrow$) If $B \subseteq A'$, then for any $g \in A$ and $m \in B$ we have $(g, m) \in I_\delta$, i.e., $g \in B'$, hence $A \subseteq B'$. □

Lemma 2 (Closure operators)**.** *The double-prime operators $\phi_G(A) := A''$ on 2^G and $\phi_M(B) := B''$ on 2^M are closures: for all $A \subseteq G$, (i) $A \subseteq A''$ (extensivity), (ii) $A \subseteq B \Rightarrow A'' \subseteq B''$ (monotonicity), and (iii) $(A'')'' = A''$ (idempotence). Analogous properties hold on 2^M.*

Proof. Extensivity: $A \subseteq A''$ follows from Lemma 1 with $B = A'$: $A \subseteq (A')' = A''$. Monotonicity: $A \subseteq B \Rightarrow B' \subseteq A'$ (antitone), hence $A'' = (A')' \subseteq (B')' = B''$. Idempotence: $(A'')'' = ((A')')'' = (A')' = A''$. The 2^M case is symmetric. □

B.2 Formal concepts as closed pairs

Lemma 3 (Characterization of concepts)**.** *A pair (X, Y) with $X \subseteq G$ and $Y \subseteq M$ satisfies $Y = X'$ and $X = Y'$ iff X and Y are closed, i.e., $X = X''$ and $Y = Y''$.*

Proof. ($\Rightarrow$) If $Y = X'$, then $X = (X')' = X''$; if $X = Y'$, then $Y = (Y')' = Y''$. ($\Leftarrow$) If $X = X''$, set $Y := X'$ so $X = (X')' = Y'$. The converse from $Y = Y''$ is symmetric. □

B.3 Lattice structure and completeness

Proposition 2 (Partial order)**.** *For formal concepts (X_1, Y_1) and (X_2, Y_2), define*

$$(X_1, Y_1) \leq (X_2, Y_2) \;:\Longleftrightarrow\; X_1 \subseteq X_2 \quad (\textit{equivalently } Y_2 \subseteq Y_1).$$

Then $\leq$ is a partial order on $\mathcal{F}_\delta$.

Proof. Reflexivity/transitivity follow from $\subseteq$. Antisymmetry: $X_1 \subseteq X_2$ and $X_2 \subseteq X_1$ imply $X_1 = X_2$, hence $Y_1 = X_1' = X_2' = Y_2$. □

Proposition 3 (Meets and joins)**.** *For any family $\{(X_i, Y_i)\}_{i \in I}$ of formal concepts,*

$$\bigwedge_i (X_i, Y_i) = \Big(\bigcap_i X_i,\ \big(\bigcap_i X_i\big)' \Big), \qquad \bigvee_i (X_i, Y_i) = \Big(\big(\bigcup_i X_i\big)'', \bigcap_i Y_i \Big),$$

and both pairs are formal concepts.

Proof. Meet: Let $X_* := \cap_i X_i$. Then $(X_*, X_*') \leq (X_i, Y_i)$ for all i. If $(Z, W) \leq (X_i, Y_i)$ for all i, then $Z \subseteq X_*$, so $(Z, W) \leq (X_*, X_*')$.

Join: Let $\tilde{X} := (\cup_i X_i)''$ (closed by Lemma 2). Then $(X_i, Y_i) \leq (\tilde{X}, \tilde{X}')$ for all i. If $(X_i, Y_i) \leq (Z, W)$ for all i, then $\cup_i X_i \subseteq Z$, hence $\tilde{X} \subseteq Z'' = Z$ and $(\tilde{X}, \tilde{X}') \leq (Z, W)$. □

Corollary 1 (Completeness)**.** *$(\mathcal{F}_\delta, \leq)$ is a complete lattice: every subset has both meet and join as above.*

B.4 Discussion of the role of α and δ

The parameter $\alpha > 0$ only rescales the logits inside σ and does not affect order-theoretic conclusions, which depend solely on I_δ. The confidence $\delta \in (0, 1)$ controls the incidence monotonically: if $\delta_1 \leq \delta_2$ then $I_{\delta_2} \subseteq I_{\delta_1}$. Thus increasing δ removes incidences and yields a different (typically coarser) concept lattice. The theorem holds for each fixed δ.

C Appendix: Proof of Proposition 1

Proof of Proposition 1. Let $D \in \mathbb{R}^{k \times d}$ have i-th row $\mathbf{d}_i^\top$ and suppose there exists $\mathbf{c} \in \mathbb{R}^d$ with $D\mathbf{c} = \boldsymbol{\tau}$. Then, for each attribute $i \in \{1, \ldots, k\}$,

$$\mathbf{d}_i^\top \mathbf{c} \;=\; (D\mathbf{c})_i \;=\; \tau_i.$$

Hence, for any object embedding $\mathbf{v}_g$,

$$(\mathbf{v}_g - \mathbf{c}) \cdot \mathbf{d}_i \;=\; \mathbf{v}_g \cdot \mathbf{d}_i - \mathbf{c} \cdot \mathbf{d}_i \;=\; \mathbf{v}_g \cdot \mathbf{d}_i - \tau_i.$$

Applying the sigmoid with sharpness $\alpha > 0$ yields

$$\sigma\big(\alpha(\mathbf{v}_g \cdot \mathbf{d}_i - \tau_i)\big) \;=\; \sigma\big(\alpha\,(\mathbf{v}_g - \mathbf{c}) \cdot \mathbf{d}_i\big)\,,$$

for all g and i, proving that $P_\alpha(m_i(g) = 1)$ is invariant under the global shift $\mathbf{v}_g \mapsto \mathbf{v}_g - \mathbf{c}$. Therefore, the soft-incidence model admits a canonical, origin-passing form without changing any probabilities or the induced incidence relation for a fixed threshold on P_α. □

Remarks. (i) The condition $D\mathbf{c} = \boldsymbol{\tau}$ is equivalent to $\boldsymbol{\tau} \in \mathrm{rowspace}(D)$. If the rows $\{\mathbf{d}_i^\top\}_{i=1}^k$ are linearly independent (i.e., $\mathrm{rank}(D) = k$) and $k \leq d$, then $\mathrm{rowspace}(D) = \mathbb{R}^k$, so a (generally non-unique) solution $\mathbf{c}$ exists for any $\boldsymbol{\tau}$. (ii) When solutions exist, they are unique up to addition of any vector in $\ker(D)$; all such choices yield the same invariance because $D(\mathbf{c} + \mathbf{z}) = \boldsymbol{\tau}$ for any $\mathbf{z} \in \ker(D)$.